Technical Report 32-1177

Surveyor III Mission Report

Part II. Scientific Results

Addendum

Prepared by:
Members of the Surveyor Scientific Investigator Teams
and Working Groups

JET PROPULSION LABORATORY
CALIFORNIA INSTITUTE OF TECHNOLOGY
PASADENA, CALIFORNIA

September 1, 1967

NATIONAL AERONAUTICS AND SPACE ADMINISTRATION

Technical Report 32-1177

Surveyor III Mission Report

Part II. Scientific Results

Addendum

Prepared by:

Members of the Surveyor Scientific Investigator Teams and Working Groups

JET PROPULSION LABORATORY
CALIFORNIA INSTITUTE OF TECHNOLOGY
PASADENA, CALIFORNIA

September 1, 1967

TECHNICAL REPORT 32-1177

Prepared Under Contract No. NAS 7-100
National Aeronautics & Space Administration

Preface

This addendum to Part II of the *Surveyor III* Mission Report contains additional scientific analyses by several members of the *Surveyor* Investigator Teams and Working Groups.

Contents

I. Chondritic Meteorites and the Lunar Surface

J. A. O'Keefe and R. F. Scott

A. Introduction

Landing dynamics and soil penetration of the *Surveyor I* spacecraft indicated that the lunar soil has a porosity in the range 0.35 to 0.45. Experiments with the *Surveyor III* soil mechanics surface sampler (SMSS) show that the lunar soil is approximately incompressible (as the word is used in soil mechanics) and that it has an angle of internal friction of 35 to 37 deg. These results point to a porosity of 0.35 to 0.45 for the lunar soil; SMSS experiments also suggest a density near 1.5 g/cm^3.

The combination of these porosity measurements, with the already determined radar reflectivity, fixes limits to the dielectric constant of the grains of the lunar soil. The highest possible value is about 5.9, relative to vacuum; a more plausible value is near 4.3. Either figure is inconsistent with the idea that the lunar surface is covered by chondritic meteorites (excluding carbonaceous chondrites) or other ultrabasic rocks. The data point to acidic rocks, or possibly vesicular basalts.

B. Porosity of Lunar Soil

It has long been known that the available measurements of the radar reflectivity of the lunar surface are sufficient to establish a functional relation between the chemical constitution of the surface and its porosity. Until recently, this relation has been used to make estimates of the porosity from assumptions about the chemical constitution. It is of even more interest to reverse the process, if possible, and to derive limits on the possible chemical properties of lunar surface material from measures of the porosity.

The landings of *Surveyors I* and *III* and the operation of the SMSS (Ref. I-1) yield information on the physical properties of the lunar surface material. When a soil is sheared, it may exhibit volume changes ranging from compression to expansion, depending on its initial state of packing. How this occurs can be recognized by visualizing the behavior of an idealized granular material consisting of spheres equal in size (Refs. I-2 and I-3). If the spheres are arranged in their closest packing state (a face-centered cubic array) and then subjected to increasing shearing stresses, the mass will expand in total volume as the spheres ride up over one another. The volume of individual spheres does not alter, but the pore volume is enlarged. Alternatively, when the medium consists of spheres in the loosest packing state (the simple cubic arrangement), the application of a shearing stress causes the total volume to decrease as the spheres slide over one another into a more stable arrangement. In the latter case, the pore volume diminishes.

Usually, the packing arrangement is characterized by a parameter termed the "porosity," n, of the medium, where

$$n = \frac{\text{Volume of voids}}{\text{Total volume}} \quad (1)$$

In the present connection, the voids referred to are those occurring between the individual grains; voids inside grains (vesicles) that do not crush during shear play no part in the volume-change behavior.

In terms of the ideal medium composed of equal spheres, the porosity at closest packing is 0.26, whereas the loosest possible packing arrangement gives a porosity of 0.48.

In real granular soil composed of irregular fragments of rock, porosities as low as 0.26 are not obtained; the lower limit to porosity is about 0.35 for a soil with a wide range of grain sizes in the closest attainable packing state. For a soil with grains smaller than a few tenths of a millimeter in diameter and essentially lacking cohesion, the porosity of the one material may range from about 0.50 in its loosest state to about 0.35 for as tight a packing as can be achieved. At the higher initial porosity, the soil will contract on shearing; at the lower initial porosity, it will expand.

When a particular soil is sheared, its volume changes (increases or decreases) until it reaches a condition compatible with the applied stress system—at which no further volume change occurs. The porosity at this constant volume state is commonly about 0.45 for low values of stress.

Following the landing of *Surveyor I*, it was concluded (Ref. I-4) that the behavior of the soil in contact with the footpads was consistent with that of a material possessing a small amount of cohesion and an angle of friction from 30 to 40 deg. The resistance of the soil in contact with the footpads was explained most plausibly in that model by a material with a density comparable to ordinary terrestrial soils, i.e., about 1.5 g/cm^3.

On the other hand, by adopting a different model of soil behavior, Jaffe (Ref. I-4) concluded from an elementary analysis of the shock-absorber strain gage records (without taking into account the dynamic behavior of the spacecraft's landing gear) that the density was lower than this, in the range 0.6 to 0.7 g/cm^3. Jaffe also found in his analysis that the mechanical behavior was best explained as that of a soil which compressed under the footpad during landing. To explain the resistance of the soil to penetration by the *Surveyor I* footpad, Jaffe (Ref. I-4) was compelled by his low value of density to assign a value of 55 deg to the angle of internal friction of the lunar soil. As Jaffe himself points out, this is much higher than values commonly observed on earth (26 to 45 deg), even in soils composed of very angular fragments. It is questionable whether such a friction angle is possible in a compressible soil of the density obtained by Jaffe because, in terrestrial soils, it is usually observed that the friction angle decreases as the porosity increases, as shown in Fig. I-1 (Ref. I-5). In Fig. I-1, each curve represents the behavior of one soil; soils with a wide range of grain sizes form the curves on the left side of the diagram, more uniform soils fall on the right.

Spencer (Ref. I-6) has made cross-sectional profiles through the rim of soil pushed up by footpad 2 of *Surveyor I*, and it is possible to use these to compare the volume of soil displaced by the footpad with the volume of the depression in which the footpad is resting. If it is assumed that no cavity exists below the footpad (an area which is not visible, of course) it is found that the volume of soil ejected is approximately equal to the volume of the depression made by the footpad (about 2,000 cm^3), within limits estimated to be $\pm 15\%$. The material was, therefore, not totally compressible, but behaved at shear in a manner similar to that of a fine-grained terrestrial soil. This

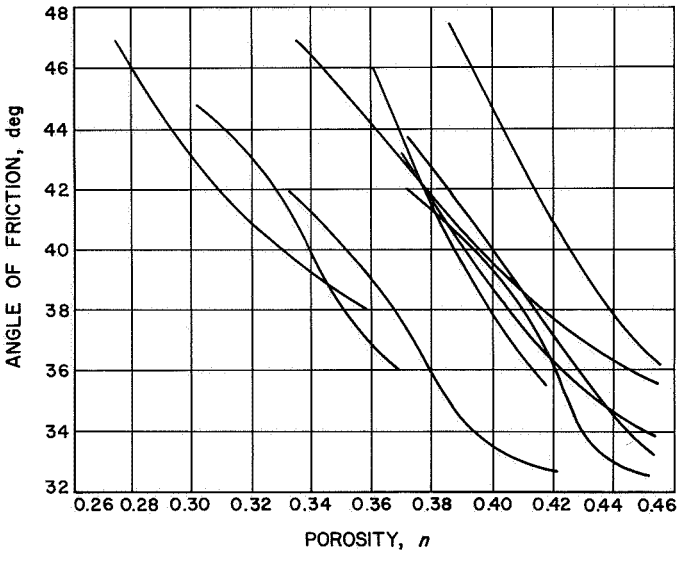

Fig. I-1. Friction angle of various soils vs porosity. Diagram was redrawn from Ref. I-5. Each curve represents behavior of one soil over range of porosities

would indicate that the lunar soil at the *Surveyor I* site possessed a porosity in essentially a normal terrestrial range of 0.35 to 0.45, excluding the volume of closed voids (vesicles) in individual grains.

In the *Surveyor III* SMSS experiment on the lunar surface, the soil's behavior again seemed to be relatively incompressible. When the SMSS was pushed into the surface in a static bearing test, the adjacent surface rose, and cracked (because of cohesion) to a distance that is indicative of the angle of internal friction of the soil. If the material were substantially compressible, it would not have exhibited the observed effects upon being subjected to a bearing test. Therefore, these conclusions contradict Jaffe's (Ref. I-4) results, indicating a compressible, low-density granular material. The reason for this appears to lie in the analysis of the *Surveyor I* landing. Jaffe calculated his value of soil density from the observation that no initial large force, which would be caused by soil inertial resistance, appeared on the strain gage record. However, a more detailed computer analysis involving the dynamics of the *Surveyor I* spacecraft's landing gear indicates that such an initial spike would not be recorded even during a landing on soil of normal density(Ref. I-7). The landing velocity is so low that the principal resistance to footpad penetration arises from the strength of the soil; the initial effect of the soil's density is almost negligible. The soil's density cannot, therefore, be calculated from an elementary analysis of the shock-absorber force history.

C. Dielectric Constant of Lunar Surface

To apply these results to the question of the chemical nature of the lunar surface, we make use of Fig. I-2, giving the relation between grain dielectric constant and bulk dielectric constant in a granular material (Ref. I-8). The relation shown here is that of Böttcher [(Ref. I-9), misspelled as "Betner" when translated by Krotikov (Ref. I-10)]. This relation is found by Gault, et al. (Ref. I-8) to provide a reasonable upper limit to the values of the grain dielectric constant as a function of porosity and bulk dielectric constant. The formula is

$$\frac{\varepsilon - 1}{3\varepsilon} = \frac{\varepsilon_0 - 1}{\varepsilon_0 + 2\varepsilon}(1 - n) \qquad (2)$$

where ε is the dielectric constant of the material in bulk, ε_0 that of the solid portion of the material.

Radar reflectivity measurements, treated on the assumption that the moon is essentially a specularly reflecting

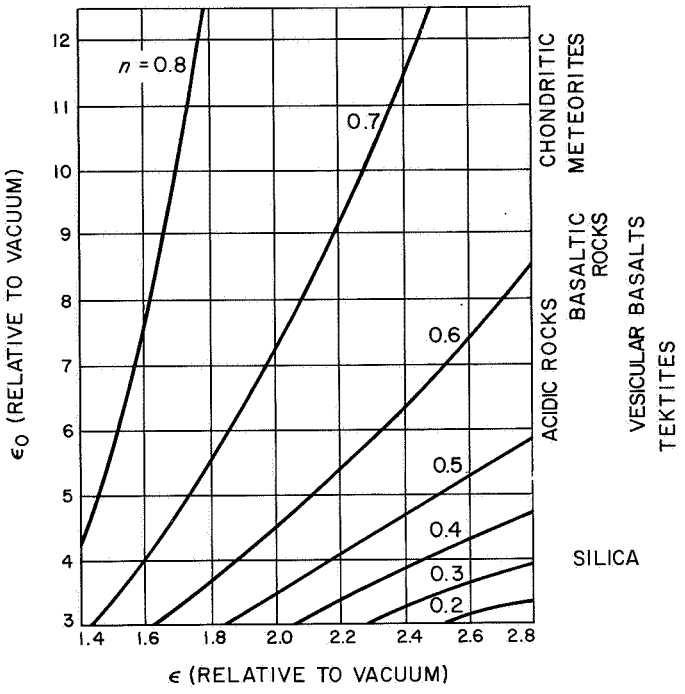

Fig. I-2. Relation between the bulk dielectric constant, ε, and the dielectric constant of the grain, ε_0, according to the Böttcher formula (Ref. I-9); n is the porosity

dielectric sphere, yield values for the bulk dielectric constant that range from 2.6 to 2.8 relative to vacuum, depending on the exact method of treatment of the small nonspecular component (Refs. I-11 and I-12). On the other hand, Hagfors (Ref. I-13), after a careful review of the problem, concludes that the radar reflections may not be coming from the surface but from a deeper layer. By this assumption, it is possible to explain the values as low as 1.6 or thereabouts, obtained from radiometric studies of the moon. We conclude that the limits 1.6 to 2.8 cover the range of the proposed values. [Brown, et al. (Ref. I-14) consider that values as high as 3.5 ± 0.7 are possible; their *theory* is not yet available and consideration of this point is probably premature at this time.]

The reflectivity *measurements* of Brown, et al. (Ref. I-14) show that the *Surveyor I* and *III* landing sites have about the same radar reflection behavior as the lunar surface in general. General theories of the lunar dielectric constant are, therefore, applicable to the particular regions whose mechanical properties were measured by these probes.

Taking 50% as an upper limit to the porosity, the highest value of the grain dielectric constant is 5.9. This value is inconsistent with the measurements on chondritic

meteorites. Because of the difficulty of measuring the dielectric constant in conducting materials, Fensler, et al. (Ref. I-15) give dielectric constants for only two chondrites (Leedy and Plainview); they did, however, also measure enough other ultrabasic rocks to give assurance that high values of the dielectric constant (7.2 or more) are associated with such rocks.

The grain dielectric constant of 5.9 is reached by stretching the data in each respect (bulk dielectric constant, conversion formula, and porosity) in favor of the hypothesis of very basic material. Using the more plausible values of 2.7 for the bulk dielectric constant (Ref. I-11), 40% for the porosity, and the Krotikov (Ref. I-9) formula

$$\frac{(\varepsilon - 1)^{1/2}}{\rho} = \frac{(\varepsilon_0 - 1)^{1/2}}{\rho_0} \tag{3}$$

where ρ is the bulk specific gravity, and ρ_0 that of the solid material, we find 4.3 as plausible for the grain dielectric constant. This would indicate either an acidic rock (granite, rhyolite, or tektite) or a vesicular basaltic rock.

The discrepancy between the maximum value of 5.9 for the grain dielectric constant and the much higher values for chondrites could be removed if we could assume that the chondritic material is highly vesicular, having 25 to 40% of the volume of the average grain occupied by void space (in addition to the intergranular voids amounting to 50% of the volume, of course). Unfortunately, it is well established that chondritic meteorites are not vesicular in this way. Some chondritic meteorites are porous, but the porosity is intergranular, not intragranular.

Conceivably, shock might produce porosity in chondritic meteorites. If this is true, and if the moon's surface is the source of chondritic meteorites, then it is to be expected that the porosity will be greatest in those pieces that have been shocked most strongly. Pieces sent off the moon will be more strongly shocked, and therefore more porous than those that have simply been knocked from one place to another on the moon. But, in fact, we find that chondritic meteorites that reach the earth are never porous; therefore, it follows that chondritic material on the moon should not be porous.

The measurements of dielectric constant thus far available do not cover carbonaceous chondrites.

Although these results are based on soil experiments at only two places on the lunar surface, the optical, radar, radiometric, and thermal data indicate that the lunar surface is much more homogeneous than that of the earth; it is likely that these experimental data are typical of the maria at least.

We conclude that the lunar maria are probably not composed, at their surfaces, of the same material as ordinary chondritic meteorites.

References

I-1. Scott, R. F., and Roberson, F., "Soil Mechanics Surface Sampler: Lunar Surface Tests, Results, and Analyses," in *Surveyor III Mission Report. Part II: Scientific Results*, Technical Report 32-1177, Jet Propulsion Laboratory, Pasadena, Calif., June 15, 1967.

I-2. Scott, R. F., *Soil Mechanics*, Addison-Wesley, Reading, Mass., 1963.

I-3. Rowe, P. W., "The Stress-Dilatancy Relation for Static Equilibrium of an Assembly of Particles in Contact," *Proc. of the Royal Soc. of London*, Series A, 269, pp. 500–527, 1962.

I-4. Jaffe, L. D., "Surface Structure and Mechanical Properties of the Lunar Maria," *J. Geophys. Res.*, Vol. 72, pp. 1727–1731, 1967.

I-5. Spencer, M. E., "The Relationship Between Porosity and Angle of Internal Friction," *Proc. 5th Int'l Conf. on Soil Mechanics and Found. Eng.*, Vol. 3, pp. 138–140, 1961.

References (contd)

I-6. Spencer, R. L., *Determination of Footpad Penetration Depth From Surveyor Spacecraft Shadows*, Technical Report 32-1180, Jet Propulsion Laboratory, Pasadena, Calif., October 1967.

I-7. Sperling, F. B., and Garba, J. A., "A Treatise on the *Surveyor* Lunar Landing Dynamics and an Evaluation of Pertinent Telemetry Data Returned by *Surveyor I*," Technical Report 32-1035, Jet Propulsion Laboratory, Pasadena, Calif., August 15, 1967.

I-8. Gault, D., Collins, R., Gold, T., Green, J., Kuiper, G. P., Masursky, H., O'Keefe, J. A., Phinney, R., and Shoemaker, E. M., "Lunar Theory and Processes," in *Surveyor III Preliminary Science Results*, Project Document 125, pp. VIII-1 to VIII-24, Jet Propulsion Laboratory, Pasadena, Calif., May 15, 1967.

I-9. Böttcher, C. F., *Theory of Electric Polarization*, Elsevier, Amsterdam, Houston, 1952.

I-10. Krotikov, V. D., "Some Electrical Characteristics of Earth Rocks and Their Comparison with Those of the Surface Layer of the Moon," *Izvestiza Vyssykh Uchebnykh Zavediniy, Radiofizika*, Vol. 5, pp. 1057–1061, 1962.

I-11. Evans, J. V., and Pettengill, G. H., "The Scattering Behavior of the Moon at Wavelengths of 3.6, 68 and 784 Centimeters," *J. Geophys. Res.*, Vol. 68, pp. 423–445, 1963.

I-12. Rea, D. G., Hetherington, N., and Mifflin, R., "The Analysis of Radar Echoes from the Moon," *J. Geophys. Res.*, Vol. 69, pp. 5217–5223, 1964.

I-13. Hagfors, T., "A Study of the Depolarization of Lunar Radio Echoes," *Radio Science* (new series), Vol. 2, No. 5, pp. 445–465, 1967.

I-14. Brown, W. E., Dibos, R. A., Gibson, G. B., Muhleman, D. O., Peake, W. H., and Peohls, V. T., "Lunar Surface Electrical Properties," *Surveyor III Preliminary Science Results*, Project Document 125, pp. III-1 and III-2, Jet Propulsion Laboratory, Pasadena, Calif., May 15, 1967.

I-15. Fensler, W. E., Knott, E. F., Olte, A., and Siegel, K. M., "The Electromagnetic Parameters of Selected Terrestrial and Extraterrestrial Rocks and Glasses," from *The Moon*, pp. 545–565, edited by Z. Kopal and Z. K. Mikhailov, Academic Press, New York, 1962.

Acknowledgment

The assistance and support of Dr. L. D. Jaffe, JPL, in the preparation of this report and the helpful advice of Dr. T. Hagfors, Lincoln Laboratories, are gratefully acknowledged.

II. Interpretation of *Surveyor III* Pictures

J. Green

A. Craterlet Origin

The morphology of many craterlets and associated rocks supports the secondary impact theory for many of the craterlets observed in *Surveyor III* pictures; however, the following origins should be considered for craterlets of the sizes shown by the *Surveyor III* camera:

(1) Direct primary impact meteoroids.

(2) Secondary impact from debris thrown out of meteoroid impact craters.

(3) Secondary impact from volcanic ejecta from volcanic centers.

(4) Maar cratering.

(5) Ebullition cratering.

(6) Lava sinks.

Interpretations of these origins are discussed in Refs. II-1 through II-4.

B. Morphology and Surface Textures of Rocks

Rocks visible in *Surveyor III* pictures range from 1 cm to more than 1 m in diameter. Some of the largest rocks observed in photographs from *Lunar Orbiters II* and *III* measure at least 25 m in diameter.[2] Worthy of statistical analysis is the observation that the smaller rock sizes (i.e., from 5 to 50 cm) may be more rounded than the angular fragments in a larger size range (more than 50 cm).

The range in rock shape is from sharply angular to subrounded, although some rock surfaces are extremely rounded. (The submerged rock in Fig. II-1, which has a suggestion of surface polish, is a good example.) The tip of a markedly angular rock fragment shown under different lighting (Day 110 vs Day 120) was inspected for dust tufting (Fig. II-2). Electrostatic charging might be expected to concentrate on points rather than curves; however, no tufting effect was observed at the 0.5-cm available resolution.

[2]E. Whitaker, personal communication.

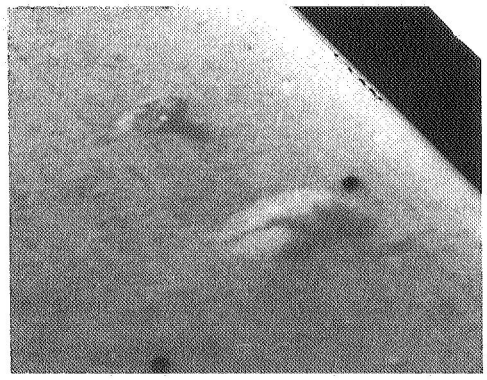

Fig. II-1. Partially submerged and rounded, cracked boulder with suggestion of glossy surface (Day 120, 14:44:53 GMT)

Fig. II-2. Absence of dust tufting on tip of pointed rock at 0.5-cm resolution (Day 110, 09:37:16)

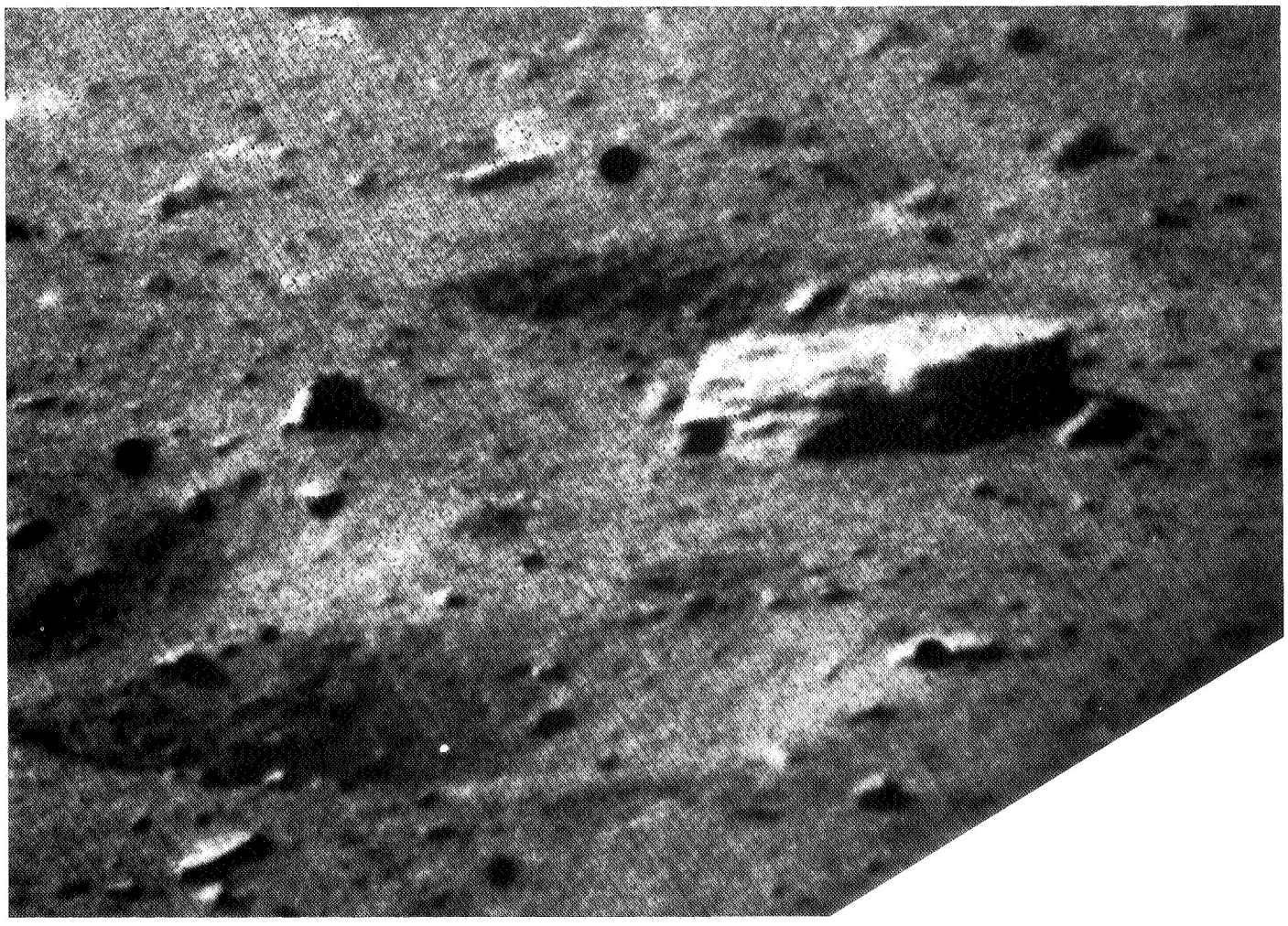

Fig. II-3. Slabby rock, about 0.5 m in length, with partings parallel to surface (Day 120, 14:52:35)

Slabby rocks, some 1 m in diameter, are visible in the pictures. One rock exhibits planes parallel to the lower and upper surfaces (Fig. II-3), although this is not always true. In some cases, dust not only forms a shallow apron around the base of the rock, but actually mantles the low points and ridges of the rock above the ground level. The top surface of this rock and others like it is not heavily coated with dust. An exception might be the pitted rock shown in Fig. II-4, in which dust occurs possibly in the pits on the sides and tops. Minor accumulations of dust might result from local secondary impacts in the surrounding soil; such dust would tend to be trapped in pits on the rock surfaces. Seismic activity associated with these impacts might be sufficient to shake off the dust from the uppermost surfaces of rocks except where trapped in pits. Poor adhesion of the lunar soil to surface rocks is demonstrated in Fig. II-5.

One of the most interesting aspects of surface rock morphology is the presence of oblate spheroid and other more elongated shapes resting on the surface with no visible evidence of indentation—almost tangential contact. Figure II-6 shows a variably mottled, oblate rock about 25 cm in length with demonstrable overhangs. The

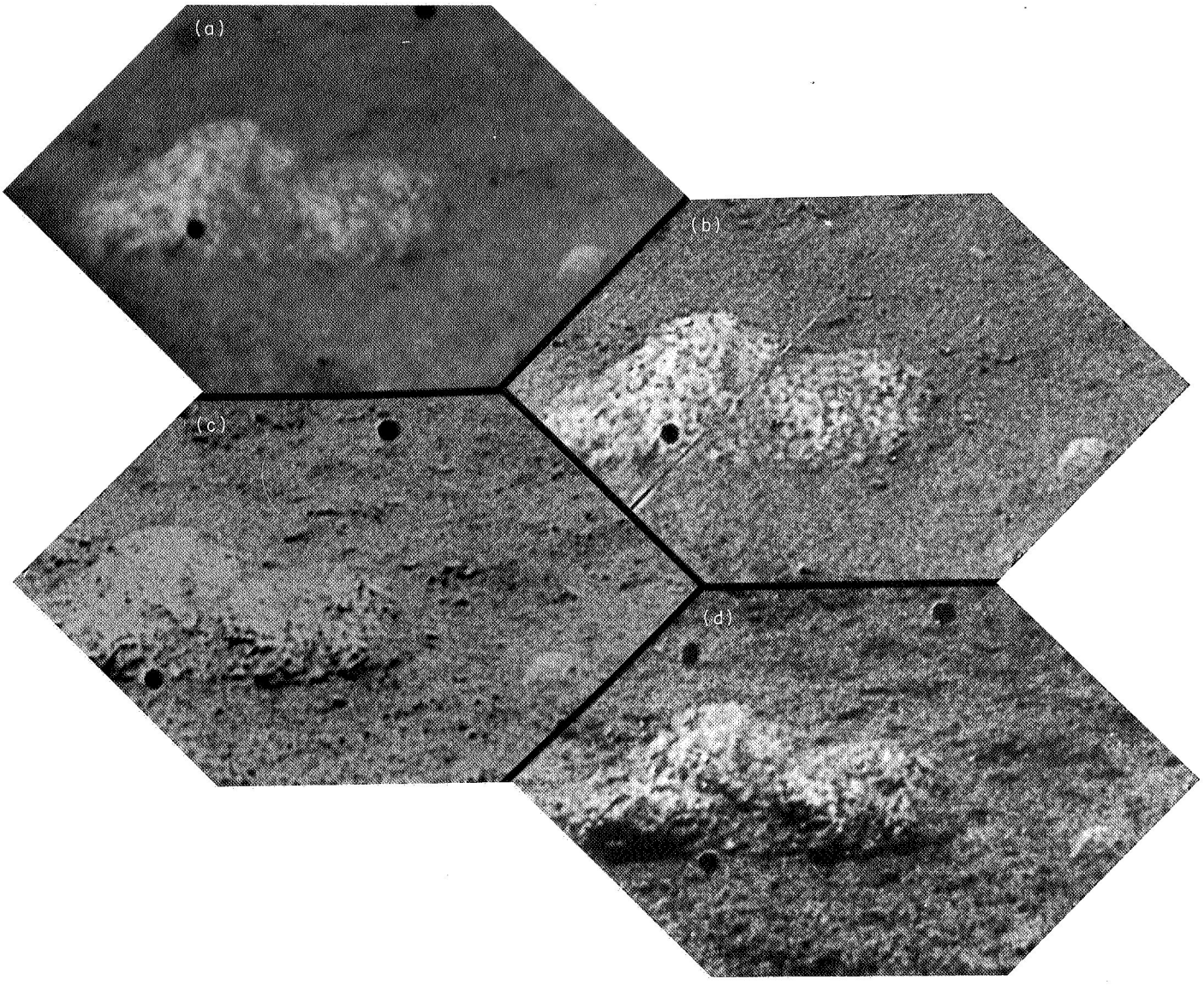

Fig. II-4. Pitted rock with possible dust in pits: (a) Day 120, 12:47:41; (b) Day 120, 12:47:41, computer-processed; (c) Day 117, 14:38:17, computer-processed; and (d) Day 116, 08:55:40, computer-processed

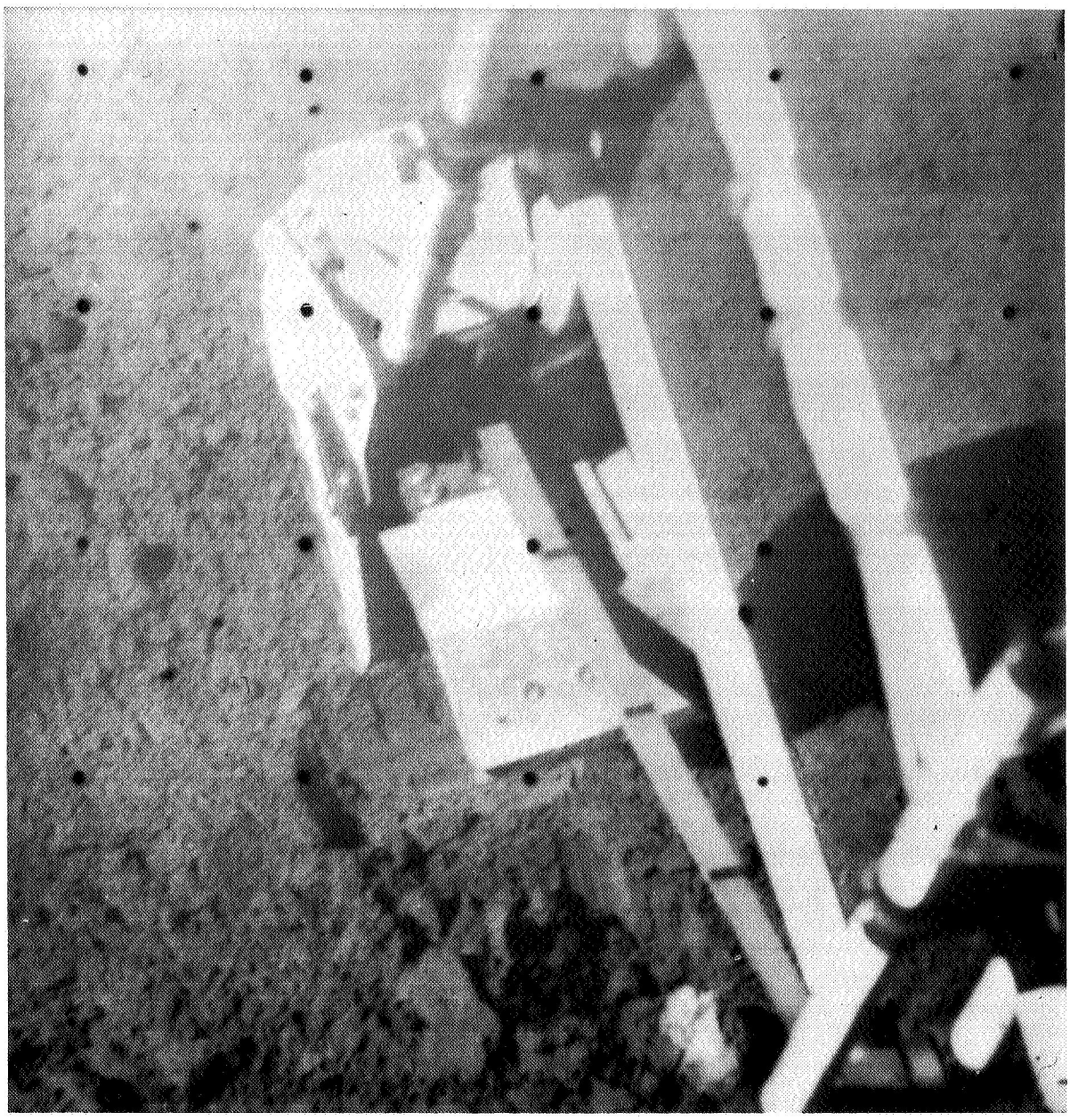

Fig. II-5. A 2-cm rock in trench made by SMSS. Note difference in albedo between rock and soil, poor adhesion of soil to rock, and faint suggestion of pitting on rock (Day 120, 17:14:20)

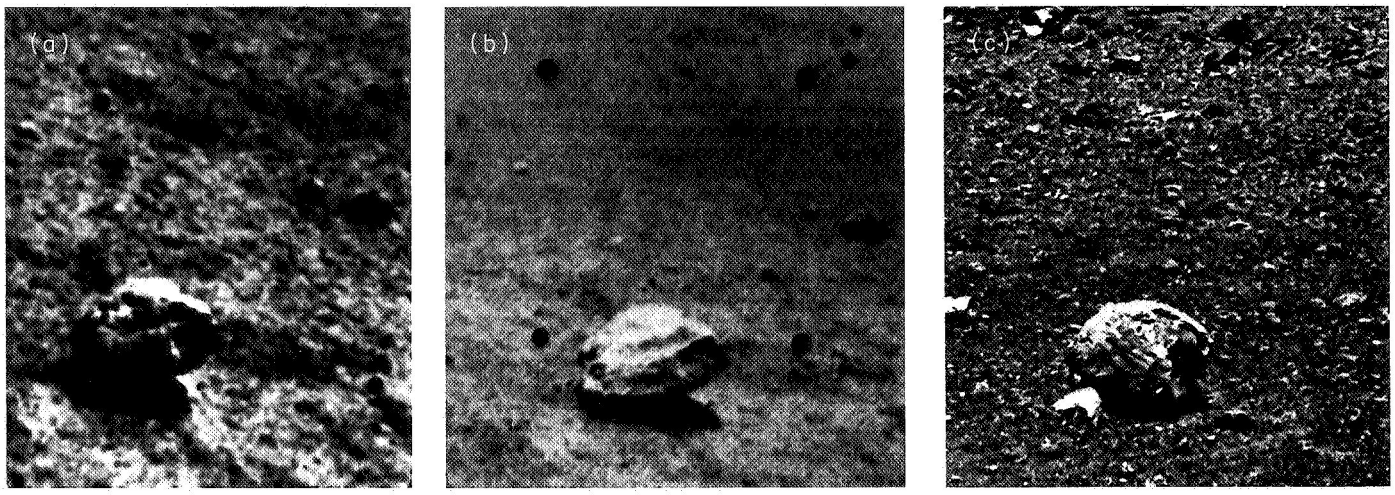

Fig. II-6. Comparison of lunar rock under two different conditions of lighting with terrestrial volcanic bomb from Hawaii: (a) lunar rock (Day 116, 09:07:06); (b) lunar rock (Day 118, 08:51:43); and (c) volcanic bomb, northern inside slope, Haleakala caldera, Maui. Lunar rock and terrestrial bomb are approximately 25 cm in length

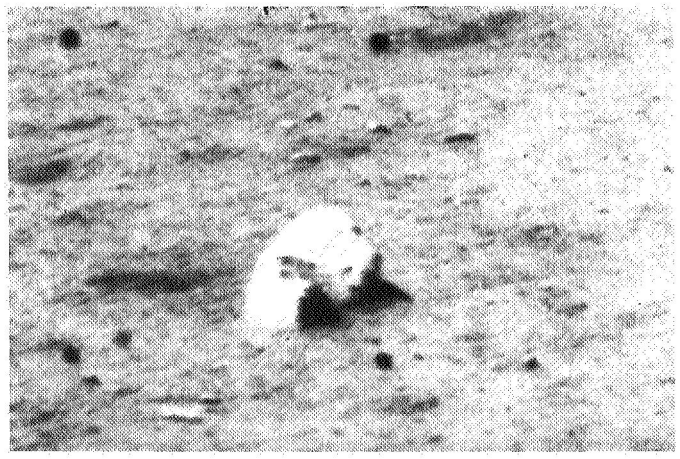

Fig. II-7. Rounded, perhaps broken, rock about 25 cm in length (Day 120, 13:42:48)

rock is ribbed and is similar in appearance to a volcanic bomb. Some rounded rocks appear to be on end, with their long axis perpendicular to the lunar surface; one rounded rock appears to have broken (perhaps on impact) and shows some pitting on the interior (Fig. II-7). Bomb-like rocks occur in some of the other pictures, which are similar to those present in the pictures from *Surveyor I*. Bomb-like rocks shown in the pictures from *Surveyor I* are compared with those from various volcanic provinces on earth in Fig. I-8.

There has been much controversy concerning the origin of pitting on lunar rocks. Vesiculation by volcanic processes, by impact melting, and pitting by small meteoroid bombardment, are three possible explanations. The rock picked up by the soil mechanics surface sampler (SMSS), with a force of approximately 3.4×10^6 dynes/cm^2 showed well-defined pits about 3 mm in diameter. A prime example of surface pitting is on the prominent rock shown under a low sun angle in Fig. II-9, although the pitting often associated with rounded rocks also occurs in many other pictures. The presence of what appears to be a partially submerged, rounded rock with surface pitting, located in a shallow crater (Fig. II-10a and II-10b), conceivably can be interpreted as a volcanic bomb in its impact crater (Ref. II-5). Other interpretations, however, must be considered.

In addition to pitting, many rocks seen in the *Surveyor III* pictures are mottled; the markings, and some appear to have positive relief, range from 1 to 5 cm in size. In one case, one mottled rock is of high albedo and conspicuously rounded. Other mottled rocks can be seen in other pictures. One of these rocks has a hint of a surface bulge or fold.

It is surprising that there was no more evidence of rock tracks caused by rolling after impact, or other secondary displacements. No slump or skid marks were observed upslope of the rock halfway down a crater slope of about 14 deg; however, one rock is associated with a faint groove.

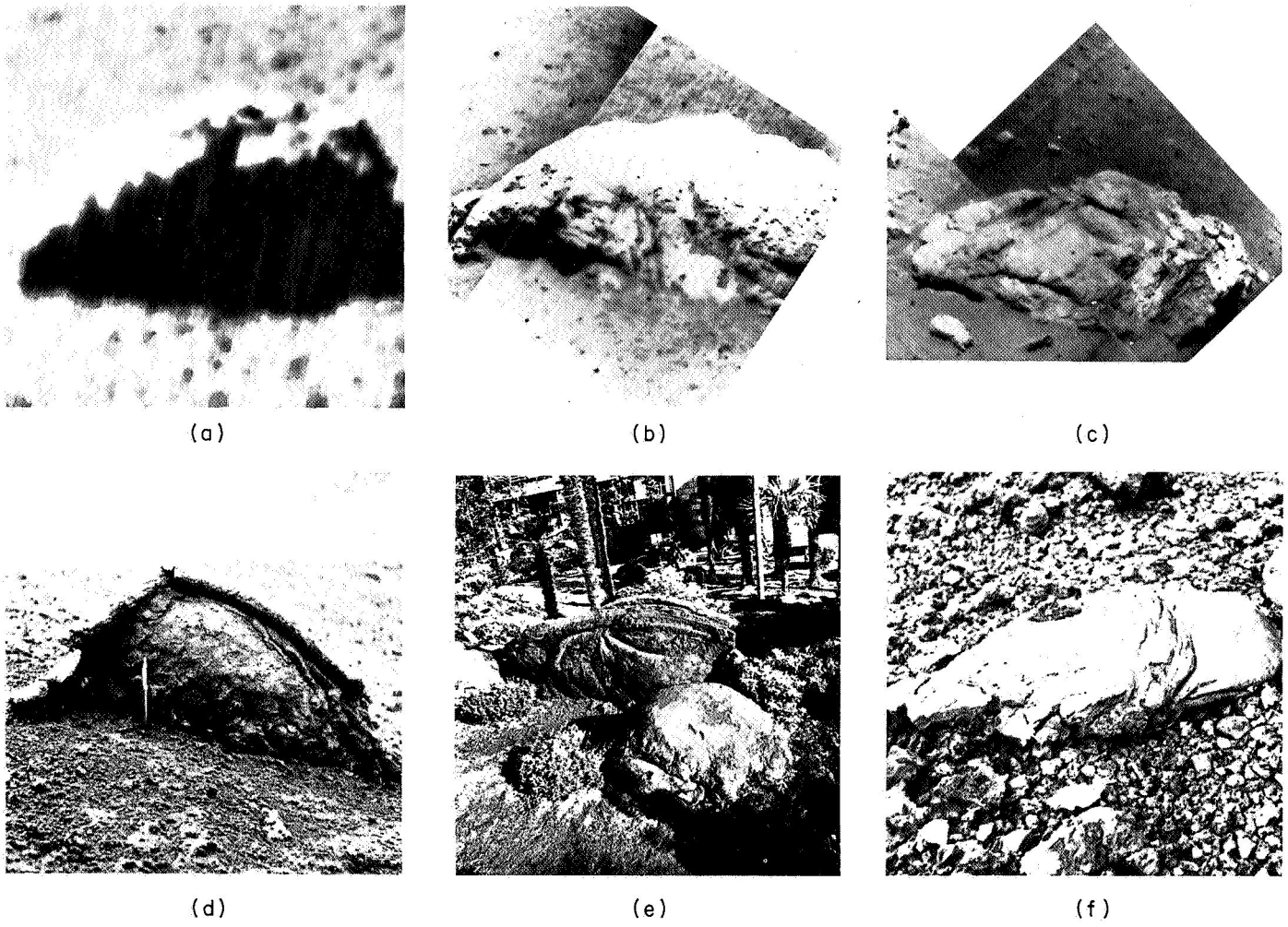

Fig. II-8. Comparison of meter-sized lunar rocks with terrestrial volcanic bombs: (a) crude suggestion of bomb-like rock in lunar picture taken by *Surveyor I*; (b) *Surveyor I* picture showing rock with surface pitting with strong suggestion of caudal appendage; (c) *Surveyor I* picture showing lunar rock with possible sag structures and suggestion of internal pitting; (d) aerodynamically shaped, basaltic volcanic bomb 0.5 m in length, Batur caldera, Bali; (e) ribbed basaltic bomb 2 m in length, Aso caldera floor Kyushu; and (f) basaltic bomb 10 cm in length, showing sag structures, Fire Mountains, Lanzarote, Canary Islands

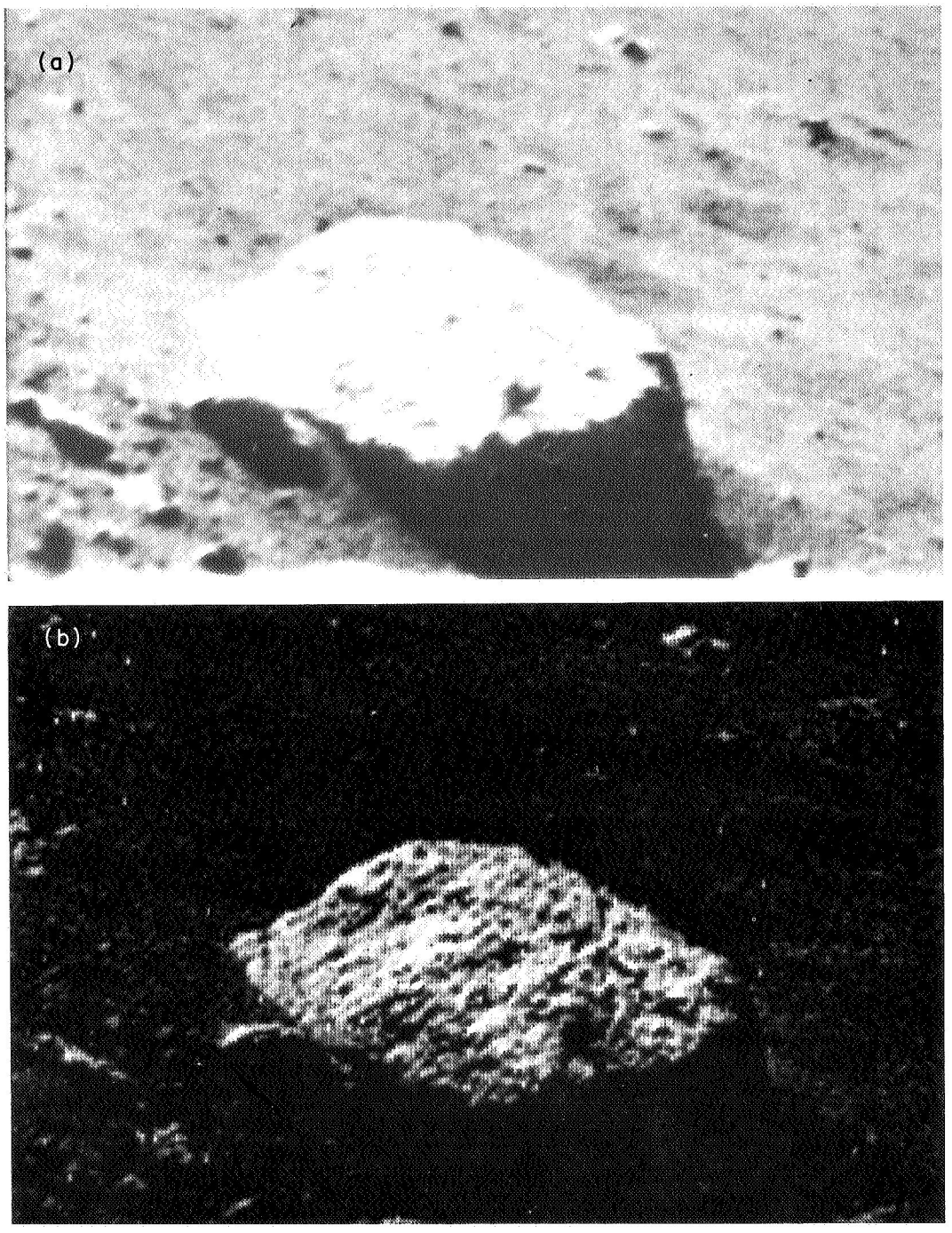

Fig. II-9. Pitted rock about 0.5 m in length: (a) Day 120, 15:07:16; and (b) Day 120, 15:07:16, computer-processed

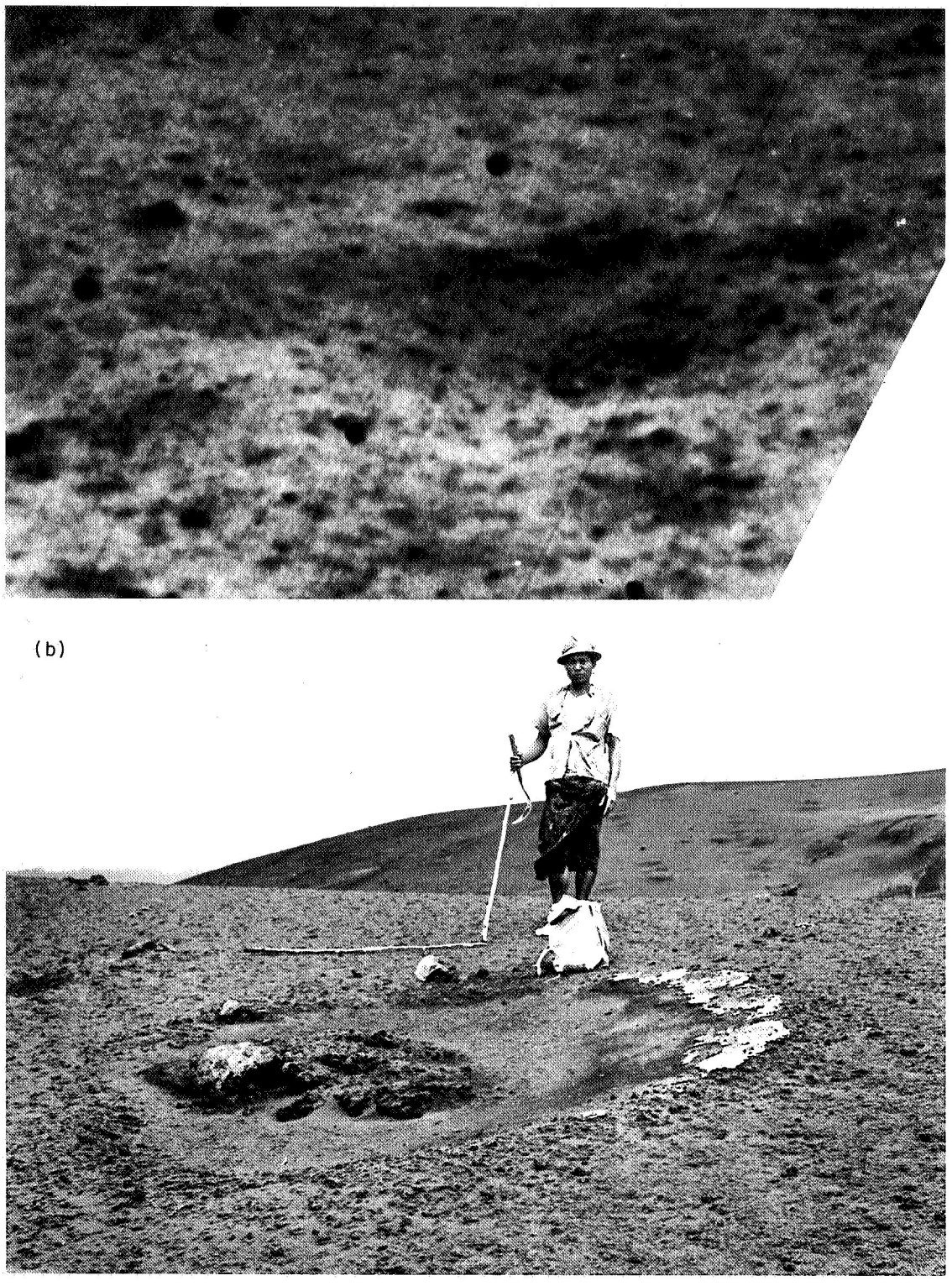

Fig. II-10. (a) Craterlet containing pitted mass (Day 116, 08:41:23); (b) volcanic bomb impact crater, central volcano, Batur caldera, Bali. Deposition of wind-blown dust in craterlet depression accounts for change in surface texture. Note other secondary impact craters on ash-covered slope in background; some of these craters have slightly raised rims

A spectrum of morphologies of early Ute Mountain quaternary basaltic rocks was photographed along the upper Rio Grande River in New Mexico (Fig. II-11) to show the range of genetically significant surface textures. The first texture is that of vesicularity. As seen in Fig. II-12, it is possible within one picture to show boulders lying side-by-side that exhibit a complete spectrum in vesicularity, even though the host rock chemistry is the same. However, in some cases, the vesicles may be extremely large and parallel to the flow layering; in other cases, bubbles produce vertical trains of vesiculation that are perpendicular to the originally vesicular horizontal flow tops and bottoms (Fig. II-13). This relationship, looked for but not found in *Surveyor III* pictures, is indicative of volcanism and not impact.

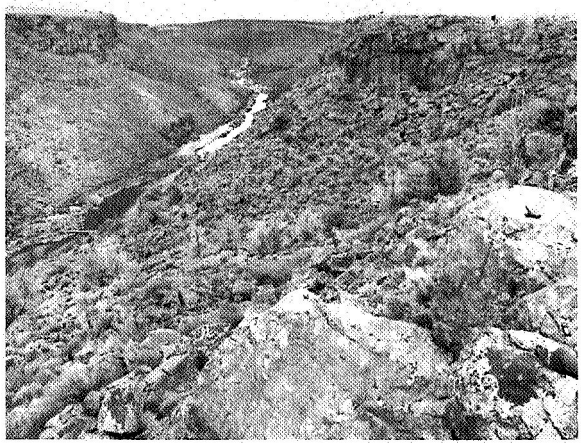

Fig. II-11. Rio Grande Gorge, near Cerro, New Mexico, Ute Mountain quaternary basalt; view looking north

Fig. II-12. Contrasting surface textures of Ute Mountain basalt boulders, Rio Grande Gorge near Cerro, New Mexico

Many of the *Surveyor III* rocks show distinct slabbiness. Sometimes vesiculation in basalts may enhance such horizontal parting (Fig. II-14); at other times, the texture is related to flow unit surfaces that are not vesicular (Fig. II-15).

As for other features of genetic significance, vesicle size increases toward the center of basaltic volcanic bombs (Fig. II-16), but not necessarily downward from a flow contact or inward from a bubble train. Breadcrusting (Fig. II-17) is a feature indicative of silicic volcanic bombs, much less so of basaltic bombs, and never of mechanically broken flow units. No rocks shown in pictures by *Surveyors I* or *III* show breadcrusting.

C. Sorting of Unconsolidated Surface Material

Of genetic significance is the absence of large and small rocks in the three SMSS jaw-cut surfaces. These cuts measure about 5 cm across by about 10 cm deep (Fig. II-18). Confining the discussion to these exposures only, one can see that the range in visible grain size is very small. In other words, from the limit of visual resolution to the width of the jaw cut, there are no fragments demonstrably larger than the 0.5-mm limit of resolution. The absence of a wide range in size of millimeter-to-centimeter rocks in the surface soil may be genetically important. This fabric is perhaps similar to the size range observed in a volcanic ash fall. Poor sorting of impact debris on the moon in the millimeter-to-meter range would probably be the case unless a high degree of subsequent comminution resulted from micrometeorites. Poor sorting of nuée ardente flows in the millimeter-to-decimeter range (Fig. II-19) would also probably occur on the moon. This would, however, apply to the lower dense phase; the uppermost surface could be well sorted and poorly consolidated.

However, the color of the subsurface material exposed by the surface sampler is dark; most ignimbrites are light colored. Also, ash flows mask other objects while ash falls mantle them. Volcanoes often emit ash within a narrow size range for sustained periods. In the *Surveyor III* pictures, a dust-mantled surface may be seen on which craterlets of probably multiple origins occur.

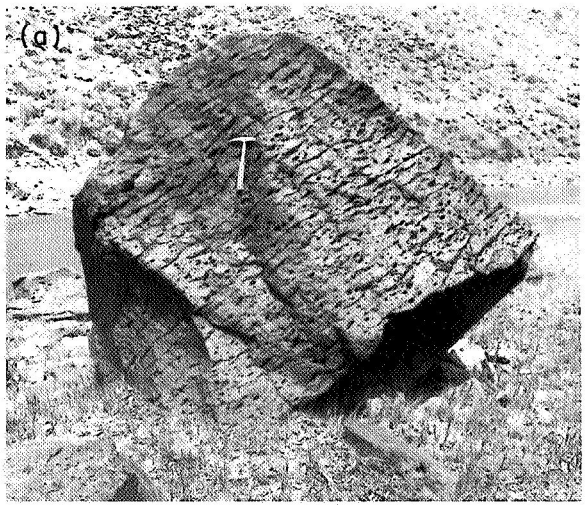

Fig. II-13. (a) Crudely layered Ute Mountain basaltic rock with large (2 to 5 cm) flow-oriented vesicles; (b) Ute Mountain basaltic rock with vertical trains of gas bubbles perpendicular to vesicular flow layer zones

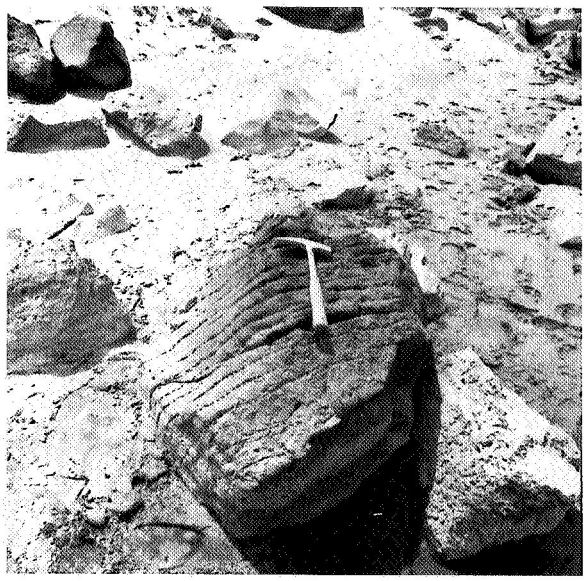

Fig. II-14. Well-layered Ute Mountain basaltic rock. Layers are defined by small vesicle concentrations

Fig. II-15. Slabby Ute Mountain basaltic rock with minor vesiculation

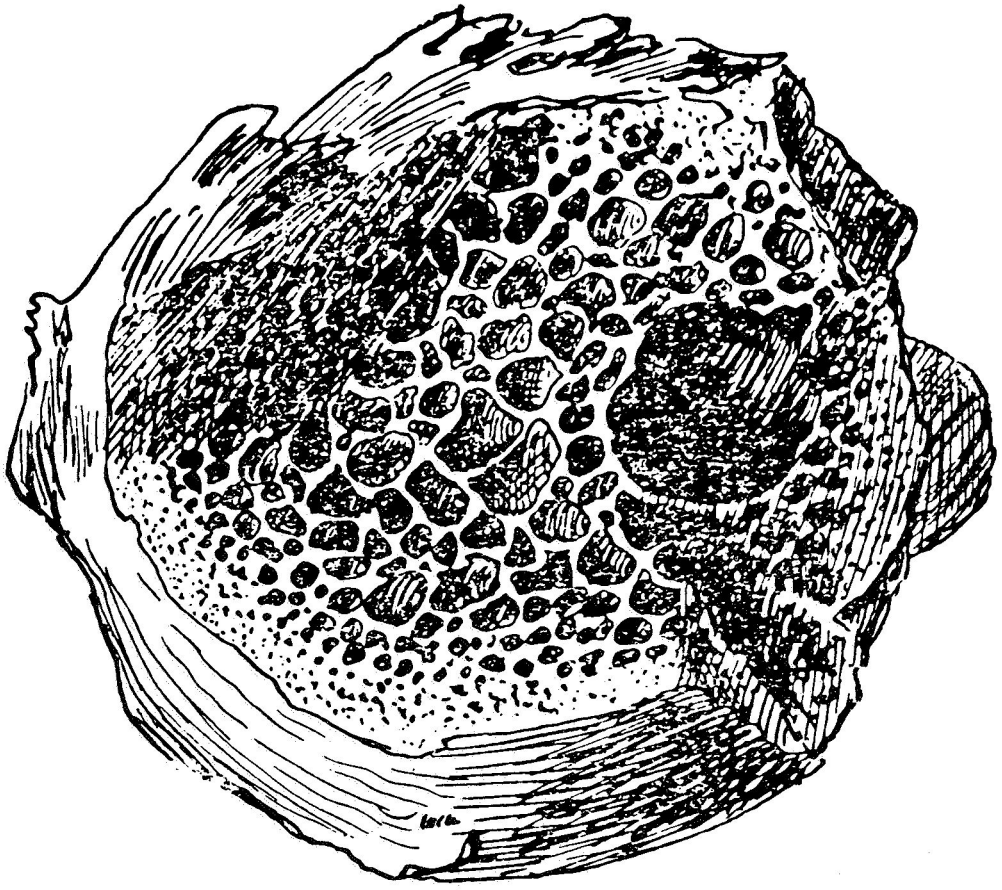

Fig. II-16. Internal structure of basaltic volcanic bomb from Kana-Mahara'ge. Diameter of the bomb is 4 cm (see Ref. II-6, p. 108)

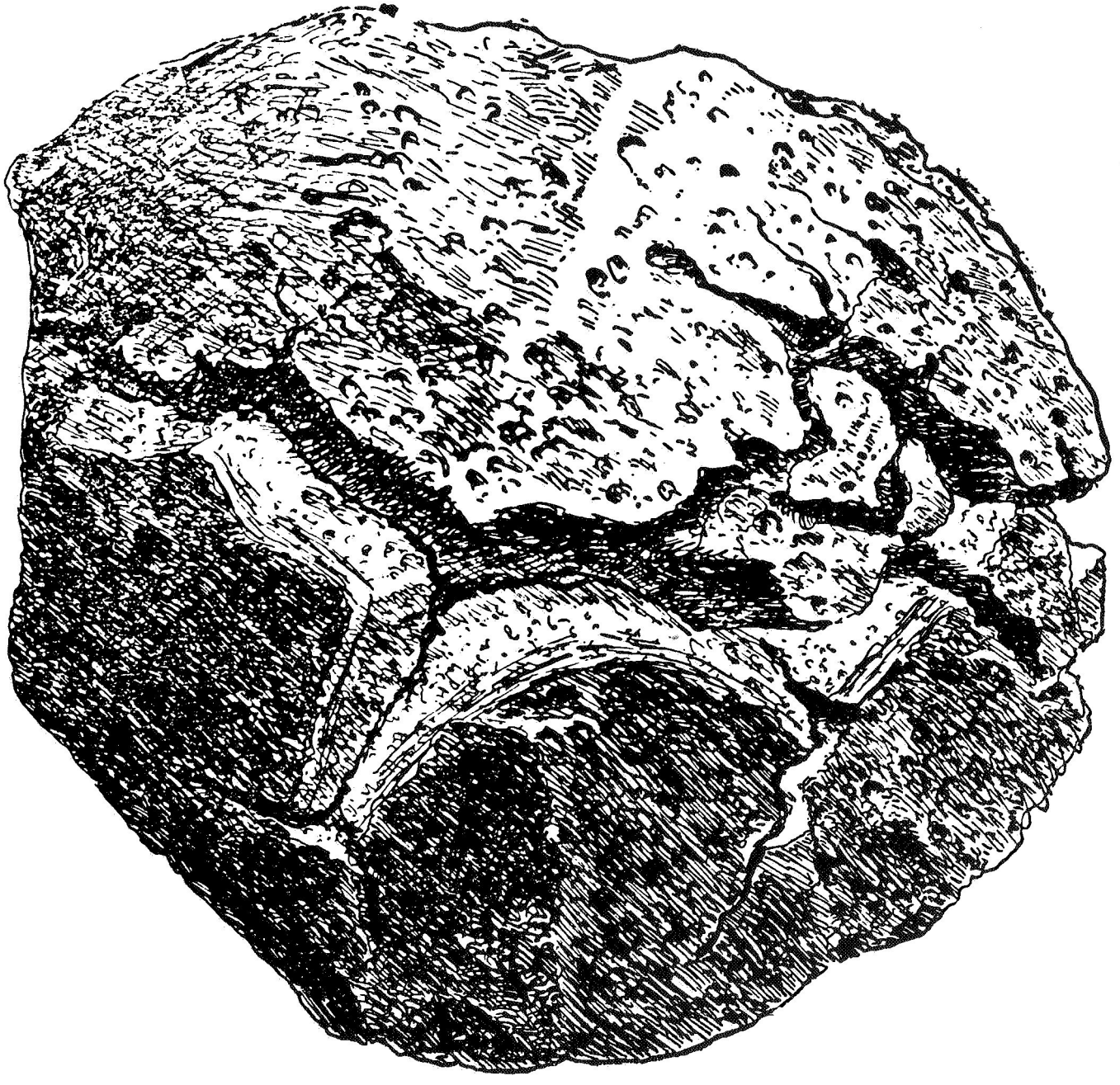

Fig. II-17. Breadcrust andesite bomb from Santorin, Greece. Diameter of the bomb is 12 cm (see Ref. II-6, p. 69)

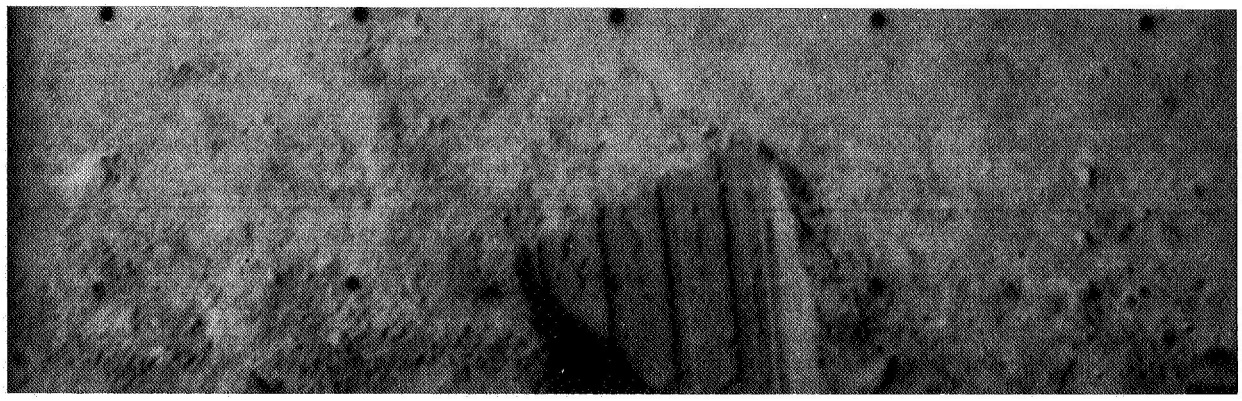

Fig. II-18. Fine grain size (less than 1 mm) of the lunar surface. The excavation (5 by 10 cm) and surface cracks in the lunar soil were made by the *Surveyor III* SMSS (Day 120, 14:28:03)

Fig. II-19. Poorly sorted ash flow at Clear Creek Canyon, Joe Lott tuff, Utah. Note the range of angularity and the variation of internal structure of included fragments

D. Nature of Unconsolidated Surface Material

The darker undersurface of the "soil" shown in pictures of the *Surveyor I* and *III* areas suggests that the uppermost surface is extremely fine-grained, as suggested in Ref. II-7. Any material pulverized to a finer grain size becomes lighter in color. The probable change in the photometric function discussed below and the appearance of uppermost surface soil platelets (some of which are tilted) on the margins of the jaw trench (Fig. II-18) or on the honeycomb "waffle" imprint help to verify a very fine grain size for this uppermost surface.

The good coherence and the poor adherence of unconsolidated lunar surface material can be interpreted in several ways. Because the likelihood of clay alteration is as remote as surface moisture at this *Surveyor* site, the clumping together of silicate grains that could have been contaminated by (1) rocket blast, (2) vaporized rock from impact, or (3) emanations from the subsurface fractures or volcanic vents can be affected by grain size, grain shape, and vacuum. There was relatively poor adherence of the soil to the SMSS scoop and to the rock shown in Fig. II-5. This suggests that grain shape is quite important in promoting coherence. If hard vacuum promotes coherence because of the grain size factor alone, then the surface dust should have adhered to a silicate rock surface. Figure II-20 shows a 0.25-mm pyroclastic basalt grain from Paricutin ash, which might be similar to the grain shape of lunar soil of equivalent size. Reduction of grain size of the particle shown would yield shards of good interlocking quality. Variations of bearing resistance with porosity for two grain sizes of Paricutin ash are shown in Fig. II-21. The high angle of repose of Paricutin ash (Fig. II-22) in the field can be attributed in large part to the high angularity of the grains (Ref. II-8).

E. Photometric Function of Uppermost Layer

Variation in the photometric function was observed on many rocks. The hint of a shiny surface on the highly rounded surface of the partially buried rock in Fig. II-1, for example, is possibly attributable to desert varnish (Ref. II-2).

The strong increase in albedo of the honeycomb imprint of footpad 2 on Day 112, compared to the days before and after Day 112, supports the concept of very fine surface dust probably below 30 μ in diameter. Some speculations are offered. First, is the uppermost surface layer genetically related to the underlying darker material, and does the surface layer coarsen with depth? If there is an increase in grain size with depth, one must be prepared to prove how a micrometeoroid turnover would preserve only an uppermost surface of much finer grain size. Volcanic ash falls commonly yield fairly well-sorted accumulations when the range of particles emitted from the volcanic vent is narrow. By hindered settling through an atmosphere, a layer of well-sorted, but very finely particulate, material is deposited on the underlying well-sorted, but coarser, material. On the moon, the possibility of separation of micron-sized ash particles from the coarser debris must not be overlooked because of the

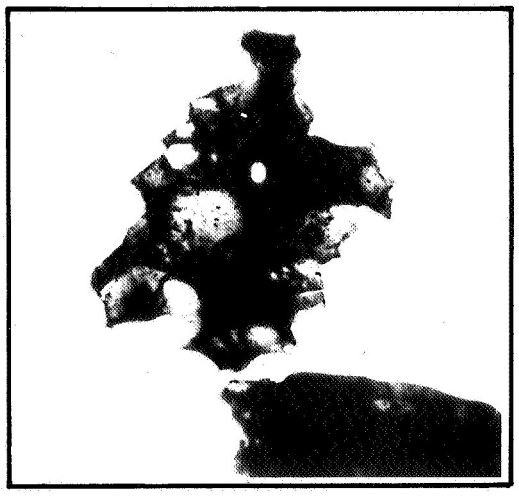

BASALTIC ASH 0.25 mm (60 MESH)

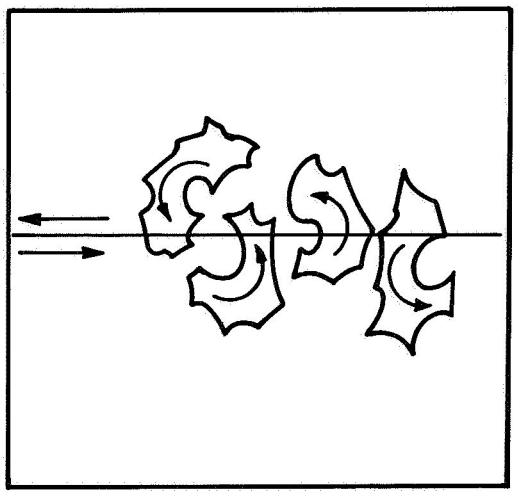

LOCKING EFFECT OF VESICULATE GRAINS WHEN ROTATED

Fig. II-20. Grain-shape effect in increasing shearing resistance. Grain shown is from Paricutin, Mexico

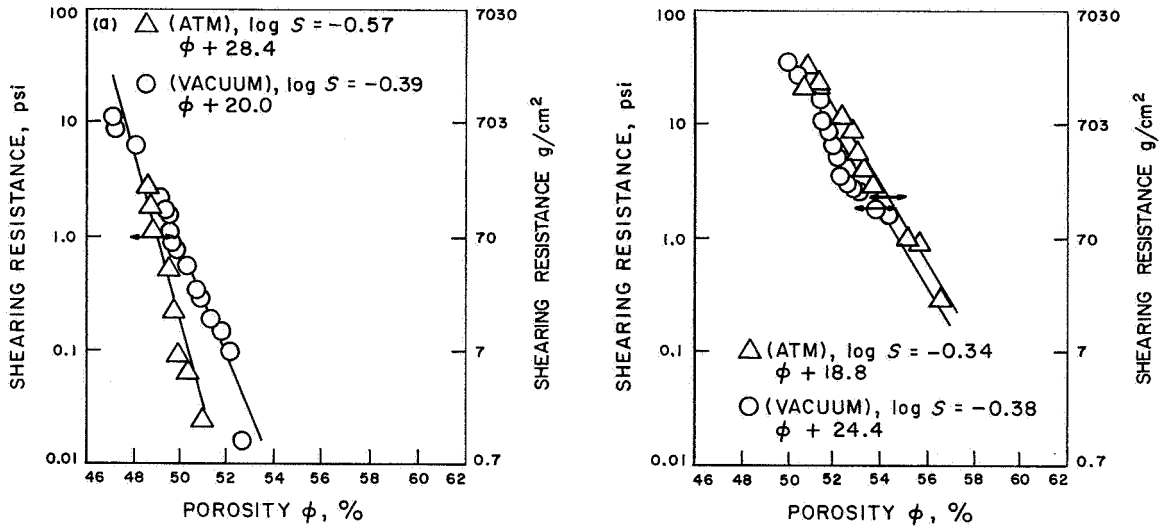

Fig. II-21. Shearing resistance vs porosity of basaltic ash of two indicated grain sizes from Paricutin, Mexico: (a) 0.10 to 0.15 mm and (b) 0.25 to 0.50 mm. Porosity at critical density is denoted by the horizontal arrow. Critical density is that density at which neither volume expansion nor contraction occurred on turning the vane penetrometer used to measure shearing resistance. The vacuum cited is 10^{-8} torr

concurrent production of volcanic gases or electrostatic charge that could have temporarily produced hindered settling.

Other materials, when crushed by footpad 2 of *Surveyor III*, also could affect the photometric function. Surface veneers on the moon may correspond to stratospheric aerosols. A study of such particles collected at an altitude of 20 km (Ref. II-9) shows that they consist primarily of ammonium sulfate. The particles have diameters ranging from 0.01 to 0.7 μ, consist of a fragile fluff, are water soluble, and have a nucleus insoluble in water. The origin of these particles by either impact, volcanic, or cosmic mechanisms has not been determined. However, on the moon, the accumulation of such aerosols is a distinct possibility. Other aerosols of a purely volcanic origin have been studied in the laboratory. McConnell, et al., (Ref. II-10) have analyzed the aerosols emitted by molten basalt at 1200°C in vacuum; the condensate contained potassium, calcium, and iron. In general, one finds abnormally high concentrations of soluble sodium compounds in fresh pyroclastics. Markhinin (Ref. II-11) has shown that when volcanic ash falls on snow, and is analyzed with the snow, the sodium is identified only in the snow water and not in the subsequent water extracts. The possibility should not be overlooked of high concentrations of sodium, sulfur, and chlorine in lunar pyroclastics in topographic low areas on the moon.

F. Conclusions

Surveyor III pictures have provided additional morphological and textural detail consistent, according to some authorities, with both the impact and volcanic models of the lunar surface. In the opinion of the writer, the data are in closer agreement with the volcanic model. If the SMSS jaw-cut exposures are representative of the upper, unconsolidated surface layer of the moon, then the formation of this fine-grained layer containing almost no visible fragments in the millimeter-to-centimeter size range suggests that the layer may be an ash fall on which subsequent events, such as volcanic explosivity, or secondary impact by volcanic bombs or meteoroid ejecta, could have occurred. Secondary impact could expose and fragment underlying bedrock. The impacting bombs and blocks could also fragment on impact, become partially or totally buried, or roll or skid to rest tangentially on the surface.

Fig. II-22. Steep standing basaltic ash cliffs, south flank of Paricutin Volcano, Mexico

References

II-1. Gault, D. E., Quaide, W. L., and Overbeck, V. R., "Impact Cratering Mechanics and Structures," Conference on Shock Metamorphism of Natural Materials, Goddard Space Flight Center, NASA, Bethesda, Md., 1966.

II-2. Green, J., "Lunar Exploration and Survival," Douglas Advanced Research Laboratories Report 4036, 1966.

II-3. Kuiper, G. P., "The Lunar Surface and the U.S. *Ranger* Programme," *Proc. Royal Soc.*, Vol. 166, pp. 399–417, 1967.

II-4. Shoemaker, E. M., "Preliminary Analysis of the Fine Structure of the Lunar Surface in Mare Cognitum," *Ranger VII. Part II: Experimenters' Analyses and Interpretations*, Technical Report 32-700, Jet Propulsion Laboratory, Pasadena, Calif., pp. 75–134, 1965.

II-5. Wentworth, C. K., "Impact Scars at Kilauea," *Pacific Science*, Vol. IX, pp. 363–369, 1955.

II-6. Reck, H., "Physiographische Studie über Vulkanische Bomben," Ergänzungsband zur Zeitschrift für Vulkanologie 1914/1915, Herausgeber: Immanuel Friededlaender, Neapel; Dietrich Reimer (Ernst Vohsen) in Berlin, Germany, 1915.

II-7. Jaffe, L., "Surface Structure and Mechanical Properties of the Lunar Maria," *J. Geophys. Res.*, Vol. 72, pp. 1727–1731, 1967.

II-8. Osgood, J. H., and Green, J., "Sonic Velocity and Penetrability of Simulated Lunar Rock Dust," *Geophysics*, Vol. XXXI, pp. 536–561, 1966.

II-9. Mossop, S. C., "Stratospheric Particles at 20-km Altitude," *Geochim. et Cosmochim. Acta*, Vol. 29, pp. 201–207, 1965.

II-10. McConnell, R. K., et al., "The Effect of the Lunar Environment on Magma Generation, Migration, and Crystallization," Arthur D. Little, Inc., Cambridge, Mass., under Contract No. NAS 9 3449, NASA, Houston, 1965.

II-11. Markhinin, Ye. K., "Pol'vulkanicheskikh Produktov v Formiro-vanii Zemnoy Kory," Izv. AN SSSR, Ser. Geol, No. 2, pp. 44–57, 1965. (Translated in *International Geology Review*, "Volcanic Products in the Building of the Earth's Crust," Vol. 8, No. 3, pp. 356–364, 1966.)